Confined variational calculations of low-energy electron-helium scattering

J.-Y. Wan,[1,2] M.-S. Wu,[1,*] J.-Y. Zhang,[1] and Z.-C. Yan[3,1]

[1]*State Key Laboratory of Magnetic Resonance and Atomic and Molecular Physics, Innovation Academy for Precision Measurement Science and Technology, Chinese Academy of Sciences, Wuhan 430071, China*

[2]*University of Chinese Academy of Sciences, Beijing 100049, China*

[3]*Department of Physics, University of New Brunswick, Fredericton, New Brunswick, Canada E3B 5A3*

(Received 10 February 2021; accepted 7 April 2021; published 19 April 2021)

The *S*-, *P*-, and *D*-wave elastic scattering of electrons by atomic helium with the scattering energy between 0.136 and 16.463 eV is studied using the confined variational method. Our calculated phase shifts improve the best published results by at least one order of magnitude. The finite nuclear mass effect on the *S*-wave phase shift at very low scattering energy between 0.022 and 0.067 eV is investigated, and the accurate *S*-wave scattering length is determined to be $1.1723a_0$, where a_0 is the Bohr radius. The results reported here can serve as a benchmark for other theoretical and experimental studies.

DOI: 10.1103/PhysRevA.103.042814

I. INTRODUCTION

The collision between electrons and rare-gas atoms has always been an important research topic, and extensive research has been carried out both experimentally and theoretically [1–15]. Scattering cross-section data are essential for understanding plasma physics, astrophysics, and radiation chemistry [1,15]. Since the electron-helium system is the simplest system, the e-He scattering provides an ideal test ground for different experimental and theoretical methods. The elastic, excitation, and ionization cross sections of this system have been extensively studied at nearly all collision energies using various approaches, such as the *R*-matrix method [4], the Kohn variational method [5], the convergent close-coupling method [16–18], and the J-matrix method [19,20]. For scattering energies below the excitation threshold, the *S*- and *P*-wave phase shifts reported by Nesbet [5] have been accepted as a benchmark until now. Therefore, we are motivated to perform an *ab initio* investigation of the e-He elastic scattering with higher accuracy for low energies.

Many experimental total cross-section sets for e-He scattering have been reported up to now [7–15,21–29], and most of them can be classified into two categories: electron-beam experiments [21] and electron-swarm experiments [26–28]. Using the hot-filament electron sources, the energy range of these beam experiments has been extended down to 100 meV. Although the electron-swarm experiments can achieve lower scattering energies, the analysis of experimental data is very complicated and may lead to large uncertainty in the cross sections [26–28]. A breakthrough was made by Shigemura *et al.* using the threshold-photoelectron source [15], in which they measured the total cross sections for the scattering energies ranging from 6 meV to 20 eV, with an electron beam energy resolution of 6–8 meV. As mentioned by Shigemura *et al.* [15], the theoretical calculation becomes very difficult due to the strong effect of electron correlation and polarization at very low energies close to the zero-energy limit, and it is also very challenging to obtain accurate experimental cross sections under the single collision condition at very low energies.

Theoretically, using the *R*-matrix method, O'Malley *et al.* [4] calculated the *S*- and *P*-wave phase shifts for e-He scattering with scattering energies from 0.136 to 16.463 eV. Nesbet [5] reported *ab initio S*- and *P*-wave phase shifts in the same energy range using the Kohn variational (KV) method, and *D*-wave phase shifts estimated using the partial-wave Born approximation formula. The *S*-, *P*-, and *D*-wave phase shifts were also investigated by Saha [30,31] by applying the multiconfiguration Hartree-Fock (MCHF) method. The most accurate *S*-wave phase shift at the momentum, $k = 0.2$ a.u., was reported by Mitroy *et al.* [6,32] using the confined variational method (CVM). The elastic cross sections below 16.463 eV were calculated by Konovalov *et al.* using the J-matrix method [19,20]. Recently, Cheng *et al.* [33] determined the *S*- and *P*-wave phase shifts in the momentum range 0.05–1.1 a.u. using the box-variational (BV) method combined with many-body perturbation theory. In their calculations, the scattering system is placed in a hard spherical wall of radius R, and the wave function satisfies the conditions $\Psi(0) = \Psi(R) = 0$. The momentum k_n can be used to determine the phase shift δ_n from the general boundary condition $j_l(k_nR) - \tan(\delta_n)n_l(k_nR) = 0$ [33,34].

The CVM approach is an *ab initio* method to study low-energy elastic scattering problems. It was originally proposed by Mitroy *et al.* [6] and applied to calculate the *S*-wave phase shift of e-He scattering. Later, this method was developed by Zhang *et al.* to study the scattering problems involving a composite projectile and target, such as Ps-H [35] and Ps-H_2 [36] scattering processes. Recently, we [37] extended the CVM to non-*S* partial waves under higher scattering energies using a different strategy to effectively eliminate the nonphysical

*mswu@apm.ac.cn

confinement effects that may occur in scattering calculations involving complex constituents.

The main purpose of this work is to extend the previous CVM calculation of e-He scattering to higher partial waves under higher scattering energies, and to provide more accurate scattering data as a new benchmark for other theoretical and experimental work. The second purpose of this work is to conduct a detailed investigation on the S-wave phase shifts of e-He scattering for the electron momentum $k \leqslant 0.1$ a.u. and then extract accurate S-wave scattering lengths for the cases of infinite and finite nuclear mass. This paper is organized as follows. In Sec. II, the CVM is introduced. The computational results are presented in Sec. III, where the S-, P-, and D-wave phase shifts with $k = 0.1$–1.1 a.u. are given in Sec. III A, the phase shifts with $k \leqslant 0.1$ a.u. as well as the S-wave scattering lengths are given in Sec. III B, and a comparison of total cross sections is presented in Sec. III C. Finally, Sec. IV is a summary. Phase shifts are expressed in radians, and atomic units (a.u.) are used throughout unless otherwise stated.

II. THEORY

A. Infinite nuclear mass

Consider the electron scattering by two potentials $V_1(\rho)$ and $V_2(\rho)$, where $V_1(\rho)$ describes the complicated interaction between the electron and the helium atom, and $V_2(\rho)$ is the model potential,

$$V_2(\rho) = \lambda e^{-0.5\rho} - \frac{\alpha_d}{2\rho^4}[1 - e^{-(\rho/5)^6}]. \tag{1}$$

In the above, λ is an adjustable parameter and $-\alpha_d/(2\rho^4)$ is the long-range polarization potential, with $\alpha_d = 1.383\,200$ being the ground-state polarizability of helium [38]. To convert a complicated scattering problem into a modified bound-state one that can be solved by applying well-established bound-state techniques, we add to the scattering potentials a confining potential $v_{\rm cp}$:

$$\begin{aligned} v_{\rm cp}(\rho) &= 0, \quad \rho < R_0, \\ v_{\rm cp}(\rho) &= G(\rho - R_0)^2, \quad \rho \geqslant R_0, \end{aligned} \tag{2}$$

where G is a tunable positive number and R_0 is chosen to be large enough so that $V_1(R_0) \simeq 0$ and $V_2(R_0) \simeq 0$.

Now let us consider the following four radial Schrödinger equations for the partial wave of total angular momentum L,

$$\left(-\frac{1}{2}\frac{d^2}{d\rho^2} + \frac{L(L+1)}{2\rho^2} + V_1(\rho) + v_{\rm cp}(\rho)\right)\phi_1 = E^s\phi_1, \tag{3}$$

$$\left(-\frac{1}{2}\frac{d^2}{d\rho^2} + \frac{L(L+1)}{2\rho^2} + V_2(\rho) + v_{\rm cp}(\rho)\right)\phi_2 = E^s\phi_2, \tag{4}$$

$$\left(-\frac{1}{2}\frac{d^2}{d\rho^2} + \frac{L(L+1)}{2\rho^2} + V_1(\rho)\right)\phi_1' = E^s\phi_1', \tag{5}$$

$$\left(-\frac{1}{2}\frac{d^2}{d\rho^2} + \frac{L(L+1)}{2\rho^2} + V_2(\rho)\right)\phi_2' = E^s\phi_2', \tag{6}$$

where $E^s = k^2/2$ is the scattering energy, and the final radial wave function is $\phi_1(\rho)/\rho$, etc. According to the boundary conditions of the scattering wave functions ϕ_1, ϕ_2, ϕ_1', and ϕ_2', their logarithmic derivatives

$$\Gamma_X(R_0) \equiv \frac{1}{X(R_0)}\frac{dX(\rho)}{d\rho}\bigg|_{R_0} \tag{7}$$

must be the same for the same E^s [6], i.e.,

$$\Gamma_{\phi_1}(R_0) = \Gamma_{\phi_2}(R_0) = \Gamma_{\phi_1'}(R_0) = \Gamma_{\phi_2'}(R_0). \tag{8}$$

Therefore, the phase shifts, determined by Eqs. (5) and (6) at E^s as a function of $\Gamma_X(R_0)$, are exactly the same.

To obtain the k- and L-dependent $v_{\rm cp}$ and V_2, i.e., the parameters G and λ, we solve the following many-body problem using the explicitly correlated Gaussian (ECG) basis [39]. We first add the confining potential $V_{\rm cp} = \sum_{i=1}^3 v_{\rm cp}(r_i)$ to the Hamiltonian of the e-He system so that it becomes a bound-state eigenvalue problem,

$$(H + V_{\rm cp})\Psi(\mathbf{r}, \mathbf{s}) = E\Psi(\mathbf{r}, \mathbf{s}), \tag{9}$$

$$H = -\frac{1}{2}\sum_{i=1}^3 \nabla_i^2 + \sum_{i=1}^3 \frac{Qq_i}{r_i} + \sum_{\substack{i,\,j=1 \\ i<j}}^3 \frac{q_i\,q_j}{|\mathbf{r}_j - \mathbf{r}_i|}, \tag{10}$$

where the nuclear mass of helium is assumed to be infinity, $\mathbf{r}_i$ and $\mathbf{s}_i$ are, respectively, the position vector and the spin of electron i, where $i = 1, 2, 3$, $\mathbf{r}$ and $\mathbf{s}$ in Eq. (9) denote collectively these variables, q_i are the corresponding electron charges, and Q is the nuclear charge. $\Psi(\mathbf{r}, \mathbf{s})$ is the eigenfunction of $H + V_{\rm cp}$ corresponding to E, where E is the total energy of the scattering system, which includes the ground-state energy of the helium atom, $E_0 = -2.903\,724\,377$ [40], and the kinetic energy of the electron, i.e., $E = E_0 + E^s$. The eigenfunction $\Psi(\mathbf{r}, \mathbf{s})$ can be expanded in terms of the ECG basis,

$$\phi_n(\mathbf{r}, \mathbf{s}) = |\mathbf{v}|^{2K_n+L}\exp\left(-\tfrac{1}{2}\mathbf{r}^{\rm T}A_n\mathbf{r}\right)Y_{LM}(\mathbf{v})\chi(\mathbf{s}), \tag{11}$$

where $\mathbf{v} = u^{\rm T}\mathbf{r}$, with $u^{\rm T} = (u_1, u_2, u_3)$ being a global vector, $\chi(\mathbf{s})$ is the spin function, and K_n is an integer. Taking the S-wave $k = 0.1$ scattering, for example, the number of basis functions used is 500, 500, 500, 500, and 600 for $K_n = 0$, 1, 2, 3, and 4, respectively. Thus, the total number of basis functions used is $N = 2600$ for the S-wave $k = 0.1$ scattering. A_n is a parameter matrix, L and M are, respectively, the total orbital angular momentum and its z component, and Y_{LM} is the spherical harmonics.

The confining parameter G is tuned to ensure that a specific total energy is yielded. For example, if the electron scattering momentum $k = 0.1$ or $E^s = 0.005$, then G is determined to be $5.011\,869\,80 \times 10^{-5}$ at $R_0 = 17$. We then solve Eq. (4) to obtain the parameter λ. Finally, the phase shift δ_L^k is obtained from Eq. (6) by applying an integration procedure and a least-squares fit between $\phi_2'(\rho)$ and $A\sin(k\rho - L\pi/2 + \delta_L^k)$ for $\rho \to \infty$.

B. Finite nuclear mass

To study the finite nuclear mass effects on scattering calculation, some modifications need to be made. After eliminating the four-body center-of-mass coordinates, the Hamiltonian

TABLE I. Convergence test of the total energy E, the electron momentum k, and the phase shift $\delta_0^{0.5}$ for the e-He scattering, as the size of basis set N increases. Infinite nuclear mass is assumed.

N	E	k	$\delta_0^{0.5}$
2000	–2.778723783	0.500001188	–0.66785
2200	–2.778724237	0.500000280	–0.66783
2400	–2.778724288	0.500000178	–0.66781
2600	–2.778724377	0.500000000	–0.66780

becomes

$$H = -\frac{1}{2}\sum_{i,j=1}^{3}\Lambda_{ij}\nabla_i\cdot\nabla_j + \sum_{i=1}^{3}\frac{Qq_i}{r_i} + \sum_{\substack{i,\,j=1\\ i<j}}^{3}\frac{q_i\,q_j}{|\mathbf{r}_j-\mathbf{r}_i|}, \quad (12)$$

where $\Lambda_{ij} = \sum_{k=1}^{4} U_{ik}U_{jk}\frac{1}{m_k}$, $m_k = 1$ in this work, and U is a 4×4 transformation matrix [39]. The coordinates r_i in the confining potential in Eq. (9) are the distance between electron i and the center-of-mass of He. Also, the reduced mass 0.999 862 963 should be used in Eqs. (3)–(6), instead of 1, where the helium nuclear mass 7294.299 536 1 is taken from [41]. Finally, for the helium polarizability α_d, we still keep the infinite nuclear mass value. The polarizability for the case of finite nuclear mass has been calculated by Bhatia and Drachman [42], and the value is 1.383 241. However, it will not change the values of the phase shifts given in the present accuracy.

III. RESULTS AND DISCUSSION

A. Phase shifts

Table I presents the convergence study of $\delta_0^{0.5}$ as the size of basis N increases. We can see that $\delta_0^{0.5}$ converges smoothly to four significant digits. In general, more basis functions are needed as k and L increase due to the increasing complexity of the wave function. In the present CVM calculations, the smallest basis set is $N = 2600$ for $\delta_0^{0.1}$ and the biggest one is $N = 3800$ for $\delta_2^{1.1}$.

Table II shows a comparison of the S-, P-, and D-wave phase shifts obtained by the present CVM, the KV method [5], the recent BV method [33], the R-matrix method [4], and the MCHF method [31], where the KV phase shifts of Nesbet have been accepted as a benchmark for other methods. Note that the KV S- and P-wave phase shifts were extrapolated using Aitken's formula with respect to the size of the basis set, and the D-wave phase shifts were estimated using a partial-wave Born approximation formula.

For the S-wave phase shifts, all the CVM values given in Table II are converged to the fourth significant digit. Compared with our results, the KV values have no more than three converged digits, and the corresponding percentage differences are 0.08% for $\delta_0^{0.1}$ and 0.48% for $\delta_0^{1.1}$. As pointed out by Cheng *et al.* [33], for $\delta_0^{0.3}$ and $\delta_0^{0.6}$ the differences between the KV and BV values are quite large. For $\delta_0^{0.3}$, the CVM value is about the average of the KV and BV values. For $\delta_0^{0.6}$, the CVM value is closer to the BV value. In general, for δ_0^{k} the percentage difference between the CVM and KV or BV values is all below 0.8%.

TABLE II. Comparison of S-, P-, and D-wave phase shifts for the e-He scattering among the present confined variational method (CVM), the Kohn variational (KV) method [5], the box-variational (BV) method [33], the R-matrix method [4], and the MCHF method [31]. Error estimates are in brackets. $a^b \equiv a\times 10^b$.

k	Present	KV	BV	R-Matrix	MCHF
			S-wave		
0.1	–0.1281	–0.1282	–0.1286	–0.1276(5)	–0.1271
0.2	–0.2650	–0.2655	–0.2657	–0.2646(1)	–0.2633
0.3	–0.4030	–0.4021	–0.4037	–0.402(1)	
0.4	–0.5380	–0.5388	–0.5387		
0.5	–0.6678	–0.6684	–0.6684	–0.671(2)	
0.6	–0.7907	–0.7930	–0.7913	–0.793(2)	
0.7	–0.9062	–0.9067	–0.9064		
0.8	–1.013	–1.0155	–1.0133	–1.018(3)	
0.9	–1.112	–1.1163	–1.1117	–1.114(3)	
1.0	–1.202	–1.2056	–1.2015		
1.1	–1.291	–1.2848	–1.2817	–1.289(4)	
			P-wave		
0.1	3.029^{-3}	3.08^{-3}	2.96^{-3}	$3.1^{-3}(1)$	3.054^{-3}
0.2	1.269^{-2}	1.311^{-2}	1.247^{-2}	$1.28^{-2}(2)$	1.2814^{-2}
0.3	2.964^{-2}	3.063^{-2}	2.929^{-2}	$2.95^{-2}(3)$	
0.4	5.390^{-2}	5.519^{-2}	5.351^{-2}		
0.5	8.449^{-2}	8.605^{-2}	8.422^{-2}	$8.3^{-2}(1)$	
0.6	0.1197	0.1209	0.1196	0.116(1)	
0.7	0.1567	0.1588	0.1572		
0.8	0.1941	0.1960	0.1947	0.189(2)	
0.9	0.2287	0.2305	0.2300	0.224(1)	
1.0	0.260	0.2626	0.2620		
1.1	0.282	0.2932	0.2903	0.281(1)	
			D-wave		
0.1	4.693^{-4}	4^{-4}	4.0^{-4}		3.85^{-4}
0.2	1.658^{-3}	1.7^{-3}	1.59^{-3}		1.637^{-3}
0.3	3.658^{-3}	3.7^{-3}	3.55^{-3}		
0.4	6.497^{-3}	6.6^{-3}	6.32^{-3}		
0.5	1.006^{-2}	1.04^{-2}	9.93^{-3}		
0.6	1.448^{-2}	1.49^{-2}	1.441^{-2}		
0.7	1.970^{-2}	2.03^{-2}	1.979^{-2}		
0.8	2.567^{-2}	2.65^{-2}	2.606^{-2}		
0.9	3.23^{-2}	3.35^{-2}	3.319^{-2}		
1.0	3.96^{-2}	4.14^{-2}	4.115^{-2}		
1.1	4.50^{-2}	5.01^{-2}	4.992^{-2}		

For the P-wave phase shifts, the CVM values for $k =$ 0.1–0.9 given in Table II are also converged to the fourth significant digit. The phase shifts for $k = 1.0$–1.1, however, are converged to the third significant digit due to near linear dependence problems when enlarging and optimizing the ECG bases. Compared with our values, the KV values have no more than two converged digits, and the percentage differences range from 0.79% for $\delta_1^{0.9}$ to 3.97% for $\delta_1^{1.1}$. The CVM values are closer to the BV values than the KV values except for $\delta_1^{0.1}$. This shows that the KV method works better for S-waves than for P-waves.

Similar to the P-wave phase shifts, the CVM D-wave phase shifts are converged to the fourth significant digit for $k = 0.1$–0.9, and to the third significant digit for $k = 1.0$–1.1, as shown in Table II. This indicates that the CVM can maintain a good performance for higher partial waves. Compared to our CVM

TABLE III. S-wave phase shifts at $k = 0.04$–0.07 for the cases of infinite nuclear mass (INM) and finite nuclear mass (FNM), and a comparison with the Kohn variational (KV) method [5] and the box-variational (BV) method [33]. The KV and BV values are obtained for the INM case.

k	δ_0^k			
	CVM (INM)	CVM (FNM)	KV	BV
0.04	−0.049190	−0.049200	−0.049256	−0.049591
0.05	−0.062190	−0.062200	−0.062065	−0.062452
0.06	−0.075139	−0.075158	−0.075035	−0.075455
0.07	−0.088227	−0.088244	−0.088148	−0.088582

results, the KV values have no more than one converged digit except for $\delta_2^{0.5}$ and $\delta_2^{0.6}$, which have two significant digits. The BV values have three significant digits for $\delta_2^{0.6}$ and $\delta_2^{0.7}$, and they have no more than one significant digit for the other cases. Nesbet [5] pointed out that the Born approximation appears to be valid within 5% for $L > 1$ in the range $k < 1.2$. From the table, however, one can see that the percentage difference between the CVM and KV values is 15% for $k = 0.1$, less than 4% for $k = 0.2$–0.9, 4.5% for $k = 1.0$, and 11% for $k = 1.1$, implying that the reliability of the Born approximation depends significantly on the scattering energy.

B. Scattering length

There are several theoretical and experimental results of the e-He S-wave scattering lengths in the literature. However, no CVM value has ever been reported, although Mitroy *et al.* [6,32] did a calculation for the S-wave phase shift at $k = 0.2$ using the CVM. The method of extracting the scattering length is to use the calculated phase shift data to fit the well-known effective range theory

$$k \cot \delta_0^k = -\frac{1}{a} + \frac{r_0 k^2}{2}, \tag{13}$$

where a is the S-wave scattering length and r_0 is the effective range. Taking into account the long-range polarization potential $-\alpha_d/(2\rho^4)$, we have the modified effective range theory [43]

$$\tan \delta_0^k = -ak\left[1 + \frac{4\alpha_d k^2}{3} \ln k\right] - \frac{\pi \alpha_d k^2}{3} + Dk^3 + Fk^4, \tag{14}$$

where D and F are two additional fitting parameters. The higher-order terms ignored in these formulas are not important for low-k scattering processes.

To extract an accurate scattering length, the S-wave phase shifts in the cases of infinite nuclear mass (INM) and finite nuclear mass (FNM) at $k = 0.04$–0.07 are calculated, and the results are shown in Table III, together with the KV and BV phase shifts of infinite nuclear mass for comparison. It is noted that the KV phase shifts are interpolated with cubic spline functions of k [5]. One of the advantages of the present method is that the Hamiltonian and its matrix elements in the FNM case preserve their functional forms under the linear transformation U appeared in Eq. (12). Thus, the extension from INM to FNM is straightforward, but computational efforts are increased. Comparing to the INM, we find that the FNM effect decreases the phase shifts, with the percentage difference ranging from 0.016% to 0.025%, which is in the order of magnitude of $m_e/m_{\rm He} = 1.3709 \times 10^{-4}$, as expected. In addition, the CVM values are closer to the KV values, with the percentage difference ranging from 0.09% to 0.2%.

TABLE IV. Comparison of theoretical and experimental e-He S-wave scattering lengths.

Method	Scattering length
Theory	
Present [INM, Eq. (13)]	1.2167
Present [FNM, Eq. (13)]	1.2169
Present [INM, Eq. (14)]	1.1724
Present [FNM, Eq. (14)]	1.1723
R-matrix (1979) [4]	1.177 ± 0.006
KV (1979) [5]	1.1835 ± 0.0059
Polarized orbital (1983) [44]	1.1575 ± 0.0579
MCHF (1993) [31]	1.1784
BV (2014) [33]	1.189
Experiment	
Drift velocity (1970) [27]	1.19 ± 0.02
Angular distribution (1975) [29]	1.172
Time of flight (1980) [25]	1.195
Time of flight (1986) [10]	1.16
Threshold-photoelectron (2014) [15]	1.194 ± 0.006

The CVM values of the scattering lengths, determined by Eqs. (13) and (14), are listed in Table IV, together with a comparison with other theoretical and experimental methods. Note that the CVM scattering lengths are extracted from the phase shifts in the range $k = 0.04$–0.07. It can be seen from the table that the scattering lengths, determined by Eqs. (13) and (14), are different at the level of 3.6–3.7 %, which indicates that the long-range polarization potential has a significant influence on the scattering length. Since the finite nuclear mass effect on the phase shift is at $m_e/m_{\rm He} = 1.3709 \times 10^{-4}$, we recommend that the S-wave scattering length is 1.1723. Our scattering length is in excellent agreement with the measured value 1.172 reported by Andrick and Bitsch [29], and is different at the level of 1–2 % compared with other measured values. Compared with other theoretical results, our scattering length is in excellent agreement with the R-matrix value 1.177 ± 0.006 [4], the MCHF value 1.1784 [31], and the KV value 1.1835 ± 0.0059 [5].

C. Total cross section

The experimental total cross sections agree very well with the theoretical calculations for the scattering energy greater than 1 eV [15]. Here we focus on the total cross section for $k \leqslant 0.1$; in other words, the scattering energy is below 0.136 eV. The total cross section can be calculated by using the partial-wave expansion

$$\sigma_t = \frac{4\pi}{k}^2 \sum_{L=0}^{\infty} (2L+1) \sin^2 \delta_L^k. \tag{15}$$

For $k = 0.1$, there is only a 0.17% difference between $\sigma_t = 20.5443\, a_0^2$, calculated by including the S-, P-, and D-wave

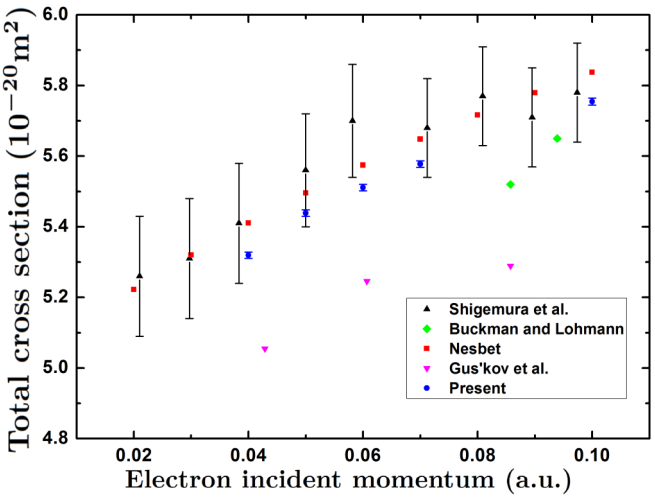

FIG. 1. Comparison of the total cross sections of e-He scattering for $k \leqslant 0.1$. Experiment: Shigemura *et al.* [15]; Buckman and Lohmann [10]; Gus'kov *et al.* [24]. Theory: Nesbet [5]; present CVM.

phase shifts, and $\sigma_t = 20.5084\, a_0^2$, calculated by including only the S-wave phase shift, where a_0 is the Bohr radius. Since the S-wave scattering will become more and more dominant in the total cross section as k decreases further, we can assume $\sigma_t \approx 4\pi \sin^2 \delta_0^k / k^2$ for $k \leqslant 0.1$ with the percentage of uncertainty less than 0.17%.

A comparison of theoretical and experimental results of σ_t for $k \leqslant 0.1$ is shown in Fig. 1. Our total cross section at $k = 0.1$ is in good accord with the experimental value of Shigemura *et al.* [15], and our values in the region of $k = 0.04$–0.07 are close to their lower limits of error bars. The results of Nesbet agree very well with those of Shigemura *et al.* for $k \leqslant 0.04$, while they have small divergences for $k > 0.04$, indicating that the tendency is opposite to our results. The experimental results of Gus'kov *et al.* [24] and Buckman and Lohmann [10] are lower than those of Shigemura *et al.* The CVM results indicate that although there have been great developments in the experimental technology of Shigemura *et al.*, the total cross sections measured at $k < 0.1$ need further improvements.

IV. SUMMARY

Using the confined variational method together with explicitly correlated Gaussian bases, the S-, P-, and D-wave phase shifts of electron-helium scattering at $k = 0.1$–1.1 a.u. have been calculated. Our well-converged calculations have improved the previous theoretical results. The finite nuclear mass effect has also been investigated, which begins to appear at the level of m_e/m_{He}. We have found that the long-range polarization potential between the projectile electron and the target helium atom has a significant influence on the S-wave scattering length. Our calculation has also confirmed the measurement results of Shigemura *et al.* [15] for the total cross section in the region $k < 0.1$ a.u.. Our definitive results presented here may serve as a new benchmark for other theoretical and experimental studies.

ACKNOWLEDGMENTS

This work was supported by the National Natural Science Foundation of China under Grants No. 11704399 and No. 11934014, by the Strategic Priority Research Program of the Chinese Academy of Sciences under Grant No. XDB21030300, and by the National Key Research and Development Program of China under Grant No. 2017YFA0304402. Z.C.Y. was supported by the NSERC of Canada.

[1] *Charged Particle and Photon Interactions with Matter*, edited by Y. Hatano, Y. Katsumura, and A. Mozumder (CRC, Boca Raton, FL, 2011).
[2] H. P. Saha, Phys. Rev. Lett. **65**, 2003 (1990).
[3] B. Bederson and L. J. Kieffer, Rev. Mod. Phys. **43**, 601 (1971).
[4] T. F. O'Malley, P. G. Burke, and K. A. Berrington, J. Phys. B **12**, 953 (1979).
[5] R. K. Nesbet, Phys. Rev. A **20**, 58 (1979).
[6] J. Mitroy, J. Y. Zhang, and K. Varga, Phys. Rev. Lett. **101**, 123201 (2008).
[7] R. W. Crompton, M. T. Elford, and R. L. Jory, Aust. J. Phys. **20**, 369 (1967).
[8] R. K. Jones and R. A. Bonham, Aust. J. Phys. **35**, 559 (1982).
[9] J. C. Nickel, K. Imre, D. F. Register, and S. Trajmar, J. Phys. B **18**, 125 (1985).
[10] S. J. Buckman and B. Lohmann, J. Phys. B **19**, 2547 (1986).
[11] V. Kumar, E. Krishnakumar, and K. P. Subramanian, J. Phys. B **20**, 2899 (1987).
[12] C. Szmytkowski, K. Maciag, and G. Karwasz, Phys. Scr. **54**, 271 (1996).
[13] W. Y. Baek and B. Grosswendt, J. Phys. B **36**, 731 (2003).
[14] S. J. Buckman and J. P. Sullivan, Nucl. Instrum. Methods Phys. Res. Sect. B **247**, 5 (2006).
[15] K. Shigemura, M. Kitajima, M. Kurokawa, K. Toyoshima, T. Odagiri, A. Suga, H. Kato, M. Hoshino, H. Tanaka, and K. Ito, Phys. Rev. A **89**, 022709 (2014).
[16] D. V. Fursa and I. Bray, Phys. Rev. A **52**, 1279 (1995).
[17] I. Bray, D. V. Fursa, and A. T. Stelbovics, Phys. Rev. A **63**, 040702(R) (2001).
[18] C. Plottke, P. Nicol, I. Bray, D. V. Fursa, and A. T. Stelbovics, J. Phys. B **37**, 3711 (2004).
[19] D. A. Konovalov, D. V. Fursa, and I. Bray, Phys. Rev. A **84**, 032707 (2011).
[20] D. A. Konovalov, D. V. Fursa, and I. Bray, Phys. Rev. A **86**, 052704 (2012).
[21] D. E. Golden and H. W. Bandel, Phys. Rev. **138**, A14 (1965).
[22] T. S. Stein, W. E. Kauppila, V. Pol, J. H. Smart, and G. Jesion, Phys. Rev. A **17**, 1600 (1978).
[23] R. E. Kennerly and R. A. Bonham, Phys. Rev. A **17**, 1844 (1978).
[24] Y. K. Guskov, R. V. Savvov, and V. A. Slobodyanyuk, Sov. Phys.-Tech. Phys. **23**, 167 (1978).

[25] J. Ferch, W. Raith, and K. Schroder, J. Phys. B **13**, 1481 (1980).
[26] L. S. Frost and A. V. Phelps, Phys. Rev. **136**, A1538 (1964).
[27] R. W. Crompton, M. T. Elford, and A. G. Robertson, Aust. J. Phys. **23**, 667 (1970).
[28] S. J. Buckman and M. J. Brunger, Aust. J. Phys. **50**, 483 (1997).
[29] D. Andrick and A. Bitsch, J. Phys. B **8**, 393 (1975).
[30] H. P. Saha, Phys. Rev. A **40**, 2976 (1989).
[31] H. P. Saha, Phys. Rev. A **48**, 1163 (1993).
[32] J. Y. Zhang, J. Mitroy, and K. Varga, Phys. Rev. A **78**, 042705 (2008).
[33] Y. Cheng, L. Y. Tang, J. Mitroy, and M. S. Safronova, Phys. Rev. A **89**, 012701 (2014).
[34] Y. Cheng, S. Liu, S. B. Zhang, and Y.-B. Tang, Phys. Rev. A **102**, 012824 (2020).
[35] J.-Y. Zhang, Z.-C. Yan, and U. Schwingenschlögl, Europhys. Lett. **99**, 43001 (2012).
[36] J.-Y. Zhang, M.-S. Wu, Y. Qian, X. Gao, Y.-J. Yang, K. Varga, Z.-C. Yan, and U. Schwingenschlögl, Phys. Rev. A **100**, 032701 (2019).
[37] M.-S. Wu, J.-Y. Zhang, X. Gao, Y. Qian, H.-H. Xie, K. Varga, Z.-C. Yan, and U. Schwingenschlögl, Phys. Rev. A **101**, 042705 (2020).
[38] Z.-C. Yan, J. F. Babb, A. Dalgarno, and G. W. F. Drake, Phys. Rev. A **54**, 2824 (1996).
[39] J. Mitroy, S. Bubin, W. Horiuchi, Y. Suzuki, L. Adamowicz, W. Cencek, K. Szalewicz, J. Komasa, D. Blume, and K. Varga, Rev. Mod. Phys. **85**, 693 (2013).
[40] H. Nakashima and H. Nakatsuji, J. Chem. Phys. **127**, 224104 (2007).
[41] P. J. Mohr, B. N. Taylor, and D. B. Newell, Rev. Mod. Phys. **84**, 1527 (2012).
[42] A. K. Bhatia and R. J. Drachman, J. Phys. B **27**, 1299 (1994).
[43] M. R. Flannery, in *Springer Handbook of Atomic, Molecular, and Optical Physics*, 2nd ed., edited by G. W. F. Drake (Springer, New York, 2006), p. 668.
[44] R. P. McEachran and A. D. Stauffer, J. Phys. B **16**, 255 (1983).